Hadronization in Nucleus by Deep Inelastic Electron Scattering

(April 28, 2003)

G.D. Cates, D. Crabb, D. Day, A. Deur, R. Lindgren,
N. Liyanage, B.E. Norum (spokesperson), O. Rondon-Aramayo,
B. Sawatzky, L.C. Smith, K. Wang (spokesperson)
University of Virginia, Charlottesville, Virginia

A. Afansasev, W. Brooks, J.P. Chen (spokesperson), J. Gomez,
D.W. Higinbotham, B. Wojtsekhowski
Jefferson Lab, Newport News, Virginia

L. Weinstein
Old Dominion University, Norfolk, Virginia

C.C. Chang
University of Maryland, College Park, Maryland

W. Bertozzi, O. Gayou, S. Gilad, B. Ma, Y. Qing, L. Wan
MIT, Cambridge, Massachusetts

S. Choi, Z.-E. Meziani
Temple University, Philadelphia, Pennsylvania

X. Jiang
Rutgers University, New Brunswick, NJ

V. Nelyubin
St. Petersburg Nuclear Physics Inst., Gatchina, Russia

S. Širca
University of Ljubljana, Ljubljana, Slovenia

K.A. Aniol
California State University , Los Angels, California

and

The Hall A Collaboration

Abstract

Semi-inclusive measurement of deep inelastic electron scattering from nuclei, $A\,(e, e'[\pi, K, p])\,X$ provides a unique opportunity to study the process of hadron formation. By comparing the electroproduction of hadrons in heavy nuclei to that in deuterium, the effects of the nuclear medium can be examined. Significant physics can be addressed using the current 6 GeV beam while, perhaps equally importantly, the direction for a broader range of future studies using the proposed 12 GeV beam can be delineated.

In order to study this process at high Q^2 one must selectively isolate such events in order to avoid being overwhelmed by the much more probable low Q^2 events. The restrictive acceptances of the Hall A HRS spectrometers are ideally suited for such selectivity. The high luminosity available in Hall A makes it possible to obtain reasonable counting rates in spite of the small cross section. Moreover, the excellent particle identification will provide data separately on pion, kaon, and proton electroproduction. The ability to observe separately the process of hadronization into different hadronic species will be very important to obtaining an understanding of the physical processes involved.

The experimental data will shed light on the mechanism of fast quark propagation in nuclear matter and the formation length of hadrons following a hard collision. The Q^2 dependence of hadron production will be a stringent test of factorization at low energy. The P_T broadening of the observed hadrons will be a signature for the rescattering of the quark inside the nuclear medium.

The measurement at $\nu = 3$ and 4 GeV will provide important input to the analysis of RHIC data.

1 Introduction

Deep Inelastic (lepton) Scattering (DIS) has played an important role in our study of the structure of the nucleon. Due to the weakness of electromagnetic interaction, the virtual photon can deliver a large amount of energy and/or momentum to a small region, to a single quark inside the nucleon without disturbing the rest of the target. As a result, a struck quark can recoil with high momentum and energy. According to QCD, quarks are confined by the color field so a struck quark must go through a fragmentation process; its momentum and energy must ultimately materialize in the form of a hadron or hadron jet.

A finite nuclear target offers a unique environment in which to study the space-time evolution of the process by which the struck quark interacts with other quarks to hadronize. In the case of a nucleon target, the quark will be more likely hadronized outside due to the small size of the nucleon. However, in the case of a large nuclear target, the struck quark or leading hadron (the one carrying the largest fraction of the momentum) must pass through and interact at varying ranges with many nuclear constituents. Consequently, the process is sensitive to the characteristics of the off-shell aspects of this interaction.

In addition to being interesting in its own right, the process studied in semi-inclusive DIS from nuclei is directly relevant to measurements being undertaken at the Relativistic Heavy Ion Collider (RHIC). There, a complex form of matter is created and exists for an instantaneously short time. Multiple quarks from the colliding nuclei interact to yield a system with a varying number of energetic quarks. The system exists for such a short time that its constituents do not reach thermal equilibrium before disintegrating into jets of hadrons. One of the principal goals of these studies is to understand the dynamics of this intermediate state. While the properties of "cold," thermally equilibrated nuclear matter are relatively well understood the density fluctuations and (assuming it can be defined) the temperature profile of such "hot" nuclear matter are not. The idea is to infer from the jet characteristics the properties of the intermediate hot nuclear state. However, in interpreting the characteristics of the hadronic jets it will be difficult to distinguish between the effects of the nuclear state from which the energetic quarks originated and those of the process by which they hadronized. The interpretation of the RHIC data will be greatly enhanced by knowledge of the quark-nuclear medium interaction best provided by DIS from nuclei.

The evolution from the leading quark to a hadron can be characterized by a formation length, Λ_h, a measure of the average distance traveled during the hadronization process. To first approximation, Λ_h can be expected to scale with ν, the energy transfered by the virtual photon:

$$\Lambda_h \approx \nu \times 1\ fm/GeV.$$

Thus, if ν is large, say 50 GeV, the quark will most likely materialize at a distance well outside even a heavy nucleus. In this case, the observed effect between the leading quark and the rest part of the nucleus has been shown to be small by the EMC[1] and TMC[2] data. However, as ν is decreased, the hadron(s) will be formed inside the target nucleus and will interact strongly with the other nucleons before leaving the nucleus. A dilution of the hadron spectrum can be expected to result.

Due to the different time scales of the hard $\gamma^* - q$ collision and the subsequent hadronization, the cross section for the entire process can be factored into the product of a factor related to the initial quark distribution and a fragmentation function. Consequently, the fragmentation function is independent of x, the Bjorken scaling variable, but scales with z, the fraction of the energy of the virtual photon carried by the hadron.

Our understanding of the space-time development of a hadronic shower, although of fundamental importance, has not progressed much beyond an elementary level. Experimental investigation has been limited by the available beams and detectors. The theoretical descriptions of quark-nucleon cross sections and hadronic formation lengths are still more qualitative than quantitative. The broadening of the transverse momentum distribution for the leading hadron due to multiple interactions of the fast quark inside the nuclear medium has been investigated [3]. It was determined that the quark energy loss can be evaluated by comparing the effect in light and heavy nuclei.

What are required are carefully controlled, high statistics measurements of deep inelastic electroproduction of hadrons from a variety of nuclear targets.

Knowledge of the momentum and multiplicity distributions of the reaction products for a variety of nuclear targets and over a wide kinematic range will be required before we can hope to have a sound knowledge of the space-time structure of a hadronic shower. As was pointed out by Bjorken [4], the space-time evolution of the final states in the parton model is important in that *it bears upon very basic questions of the dynamics of deep inelastic process. Looking in detail at the space-time evolution of the process, say in electroproduction, from the time when the quark is hit to the time when the final hadrons emerge as asymptotic states one should learn something about the dynamics of confinement.* For this purpose, the *A-dependence of the spectrum of energetic hadrons produced in electroproduction could turn out to be quite interesting.*

High quality semi-inclusive data will be crucial to interpreting the RHIC [5] data in terms of quarks propagating in a high temperature and high density environment. Lattice gauge calculations indicate that a phase transition may occur from hadronic nuclear matter to a color deconfined medium (quark-gluon plasma) in relativistic heavy ion collisions[6]. Data from RHIC[7] have shown a jet quenching effect in the dense plasma. The quenching manifests itself as a suppression of the P_T spectra in A-A collisions compared to p-p collisions. The effect becomes significant near $P_T = 4$ GeV/c, kinematics which correspond to the case of $\nu = 4$ GeV achievable at Jlab. Although jet quenching in central heavy ion collisions can be described qualitatively by the scattering of a parton in a dense medium, it is necessary to understand other nuclear medium effects before quantitative conclusions can be drawn [8]. In this regard, the measurement at Jlab will provide valuable insight.

In QED, Bremsstrahlung radiation is suppressed relative to the Bethe-Heitler formula when the radiation formation time is long compared to the mean-free path; this is the LPM (Landau-Pomeranchuck-Migdal) effect [9] [10]. It has been shown that specific non-Abelian effects influence the detailed interference pattern in the case of QCD [11] [12]. The LPM effect is very important in the energy loss calculations for a parton traversing dense QCD matter as in RHIC. This effect could be seen and studied by comparing data from $\nu > Q^2$ to $\nu < Q^2$ under the kinematic conditions of the proposed experiment.

In proposing to study hadronization associated with DIS at relatively high Q^2 at Jlab, one is faced with two constraints. The first one arises from the relatively low beam energy. Inevitably, an overwhelming number of the electron events will correspond to low Q^2's, since the cross section is proportional to $1/Q^4$. To suppress this high rate component one must employ a spectrometer with small energy and, hence, angular acceptance. This will offer unique sensitivity to a narrow, high Q^2 range. A Hall A High Resolution Spectrometer (HRS) is ideal for this. The high luminosity possible in Hall A compensates for the small acceptance and makes such a selective measurement feasible.

The second challenge relates to the hadron-arm. For current fragmentation, we have to select those hadrons with large z, $z > 0.5$; that is, hadrons with higher momenta. As is the case with the scattered electrons, the momentum distribution of the emitted hadrons is largest for low momenta. To preferentially select high momentum hadrons one must locate a limited acceptance detector along the virtual photon direction. Therefore, the combination of the two HRS spectrometers in Hall A, HRSR for the scattered electrons and HRSL for the leading hadrons, constitutes a good solution for a study of current fragmentation at high Q^2 at Jlab.

The distinctive particle identification (PID) of the HRS will add an important feature to the experiment. Comparing the measurements of pion, kaon, and proton electroproduction will allow hadronization into different hadronic species to be compared.

We propose to study nuclear effects in the process of hadronization in semi-inclusive DIS via the reaction $A\,(e, e'[\pi, K, p])\,X$ using a 6 GeV beam and several kinematic settings. Four targets will be used: deuterium, carbon, copper and tungsten. The HRSR will be used to detect electrons and HRSL will be used to detect hadrons (pion, kaon, and proton). The ν and z-dependence of the ratios of the fragmentation functions for $A > 2$ to that for deuterium will be a measure of the formation time of the hadronization; the Q^2 and ν dependence will show possible signatures of LPM effect. The data from different P_T coverage will enable one to evaluate the multiple scattering of fast quarks inside nuclei. Information from the proposed experiment will also serve as an important input to the analysis of RHIC data.

2 Physics Motivation and Formulation

2.1 DIS and Current Fragmentation

For inclusive inelastic scattering , individual events are characterized by the variables of ν and Q^2. The cross sections are parametrized in terms of the structure functions W_1 and W_2. The differential cross sections is [13]

$$\frac{d^2\sigma}{dQ^2 d\nu} = \frac{4\pi\alpha^2 E_1}{Q^4 EM}[W_2(Q^2,\nu)\cos^2\frac{\theta}{2} + 2W_1(Q^2,\nu)\sin^2\frac{\theta}{2}],$$

where Q^2 is the negative four-momentum transfer squared,

$$Q^2 = -q^2 = 4EE_1\sin^2\frac{\theta}{2},$$

$$\nu = E - E_1,$$

E is the incidental electron energy on a target with mass M, and E_1 is the electron energy after the scattering at a laboratory angle θ,

$$E_1 = \frac{E - \frac{W^2-M^2}{2M}}{1 + \frac{2E}{M}\sin^2\frac{\theta}{2}}.$$

W is the invariant mass of the virtual photon and the target nucleon system,

$$W^2 = M^2 + 2M\nu - Q^2.$$

At higher Q^2 and ν, inelastic scattering leaves the target in a continuum state. Under these conditions the scaling functions $F_1 = W_1(Q^2,\nu)$ and $F_2 = \frac{\nu}{M}W_2(Q^2,\nu)$ are nearly independent of Q^2 and are directly related to the parton densities within the nucleon. In this Bjorken scaling region the DIS cross section can be expressed as [14]

$$\frac{d^2\sigma}{dxdy} = \frac{8\pi\alpha^2 ME}{Q^4}\{F_2(x,Q^2)[1-y] + xy^2F_1(x,Q^2) - \frac{M}{2E}xyF_2(x,Q^2)\},$$

where the Lorentzian invariant quantity x is the Bjorken scaling variable

$$x = Q^2/2pq = Q^2/2M\nu,$$

and

$$y = \nu/E.$$

According to the scaling theory, the structure functions at fixed x depend strongly on x, but only weakly on Q^2. This implies that the nucleon is composed of nearly free point-like partons and the structure functions are related to the momentum densities of the partons within the nucleon.

For semi-inclusive hadron production (only one hadron detected), the hadron fragmentation function is defined as [15]

$$D^h(x, Q^2, z, p_T^2) = \frac{1}{\sigma(Q^2, x)} \frac{d^2\sigma^h}{dz dp_T^2}$$

where

$$z = \frac{E_h}{\nu}$$

is the fraction of the virtual photon energy absorbed by the hadron. P_T is the transverse (to $\vec{q}$) momentum of the detected hadron.

According to the quark model, the virtual photon is absorbed by a quark in a short time. Then, the struck quark undergoes a fragmentation process of longer duration to form a hadron. Hence, the fragmentation function can be factorized into [15]

$$D^h(x, z) = \sum_q \epsilon_q(x) D_q^h(z),$$

where ϵ_q is the probability for a quark of type q to be involved in fragmentation, and

$$\epsilon_q = e_q^2 q(x) / \sum e_q^2 q(x),$$

where $q(x)$ is the probability that the quark q with charge e_q has a momentum fraction in the range from x to $x + dx$. D_q^h is fragmentation function describing the production of a hadron h from the quark q. D_q^h describes the distribution of semi-inclusive hadron per scattered electron. According to the scaling hypothesis, ϵ_q and D_q^h are independent of Q^2 and, moreover, D_q^h is independent of x but scales with z.

After summing over P_T^2, [16]

$$D^h(x,z) = \frac{1}{\sigma_{tot}}\frac{d\sigma^h}{dz} = \frac{1}{N_e}\frac{dN^h}{dz},$$

where N_e is the event number of DIS, and N^h is the number of detected hadrons of type h.

According to jet universality, lepton scattering from a parton in a nucleon N contains the same information as electron-positron annihilation into an N-$\bar{\mathrm{N}}$ pair. However, unlike the annihilation reaction, lepton scattering on a fixed target offers a unique way to study the fragmentation of compound quark states such as a di-quark. As the struck quark recoils, initiating a fragmentation event, the rest of the nucleon will move reciprocally, undergoing a spectator or target fragmentation. Target fragmentation can be separated from quark fragmentation by considering the Feynman scaling variable x_F, defined by

$$x_F = P_L^*/P_{Lmax}^*,$$

where P_L^* is the longitudinal momentum component of the hadron with respect to the virtual photon direction in the center mass system, the maximum value of which is given by

$$P_{Lmax}^* = W/2.$$

Fragmentation of the struck quark is formed in the region of positive x_F, while target remnant favors negative x_F.

Current fragmentation can be depicted in the Breit frame, where the virtual photon is completely space-like with four-momentum $(\vec{P}, E) = (0, 0, -2xP, 0)$. Here, P is the momentum of the nucleon and xP is the momentum of the leading struck quark. After the collision, the struck quark carries a four momentum $(0, 0, -xP, 0)$ along the virtual photon direction. Hence, $Q = 2xP$ or $P = Q/2x$. The picture in Breit frame is an approximation to the case when transverse momentum of the quark is negligibly small compared to its total momentum or, equivalently, $P >> P_T$. By placing the hadron arm in the direction of $\vec{q}$ we will select those hadrons with low P_T, thus optimizing the conditions for a study of current fragmentation. Comparing data at different Q^2 and ν will provide an examination of factorization.

2.2 Motivation

In DIS, a quark absorbs an energetic virtual photon and recoils along the direction of the photon. After a short distance it will materialize into a hadron or a hadronic jet. Both the quark and the hadron(s) will interact with the nuclear medium during this time. The interaction cross section for a hadron is typically about 20 mb, while the cross section for the quark is much smaller. Varying the length of the path of the quark inside the nucleus will provide a measure of the formation length in hadronization. By comparing the attenuation observed in different nuclear targets to theoretical models one can expect to learn much about processes inside the nuclear medium.

The proposed experiment will focus at higher Q^2's where the quark degree of freedom will be dominating against coherent process. As we view DIS from a frame with high momentum, the life time of a free quark is dilated as $\gamma\tau$, while the size of the nucleon is shorten as $1/\gamma$, hence a free quark is more probable to be probed. At high Q^2, the influence of the nucleon degree of freedom will be smaller due to a stronger Lorentzian boost. We will study current fragmentation at two Q^2's with similar ν, as well as two ν's at the same Q^2, which can be used to test a possible effect which are sensitive to the kinematic changes.

The data at low ν can be expected to show a larger nuclear effect, since the hadron is formed in a shorter time, and the hadron needs to travel a longer distance in the nucleus. At the low ν sizable effect can be seen even with a medium sized target nucleus. The data will also be used to study the relation between the formation time τ_h and ν.

The results of hadron attenuation as a function of z can be used to project the z-dependence of the formation time τ_h which is determined by the QCD dynamics of hadron formation. In ref. [17], a few different parameterizations are listed:

$$\tau_h = z\nu,$$

$$\tau_h = (1 - z)\nu,$$

and

$$\tau_h = (1 - \ln(z))z\nu.$$

Clearly, these various models will predict different shapes for the z-dependence. Using different dynamical models, one could obtain suppression of τ_h either at small z [18] or at large z, as in the gluon bremsstrahlung mechanism [19]. Data from the proposed experiment will be used to constrain the z-dependence.

Since the transverse momentum of leading hadron or the struck quark is an initial state property, any observation of a broadening of P_T will reflect the multiple scattering of the quark inside the nucleus. Comparing the data to theory [3], a measure of the energy loss by the quark can be derived. A theoretical review of this subject can be found in [20]. The energy loss results from both collisional and radiative losses. Due to the large momentum involved, coherent processes may strongly influence the radiative process in a way similar to that observed in QED processes. It is important to understand the coherent aspect of QCD multiple scattering in order to interpret data from heavy ion collisions. The medium effect of gluon radiation is expected to be maximal around 1 GeV to 4 GeV. Jlab data with ν of 3 GeV to 4 GeV will play a major role in this investigation. [21]

The initial photon-quark interaction will be largely independent of the nuclear target while the hadronization processes will be significantly affected by the amount of nuclear matter the struck quark and/or hadron(s) must pass through. Accordingly, these processes alone can be expected to exhibit an A-dependence. A combination of all these dependencies will help clarify the issues related to the dynamic process of hadronization.

3 Previous Experimental and Theoretical Work

3.1 Experimental Data

Nuclear effects on hadronization were first studied using DIS by Osborne *et. al.* at SLAC [22]. The electron beam energy was 20.5 GeV, the targets were liquid hydrogen, deuterium, Be, C, Cu and Tn. Q^2 ranged from 0.35 to 5.0 $(\mathrm{GeV/c})^2$, while W^2 was between 7 GeV^2 and 31 GeV^2, P_T was less than 1.0 GeV/c, and x_F was positive. The data showed that there was an attenuation of forward going hadrons and that the attenuation increased with the atomic number A of the target nucleus. A magnet dipole was used to separate particles by charge but no particle identification was performed. Despite limited statistics (10 k event/target) the results were quite interesting, since they revealed nuclear effects in the process of hadronization. In addition, this experiment demonstrated that the spatial evolution of hadron formation can be studied by semi-inclusive DIS.

Similar experiments subsequently were performed at CERN (EMC) [1] using muon beams with energies up to 175 GeV and targets such as C, Cu and Sn. It was found that at such energies, the struck quark is largely decoupled from the target nucleus, leaving it and then hadronizing outside the nuclear medium. Combining the experimental results from SLAC and CERN, it can be surmised that nuclear effects are more important when ν is small. Thus, they are more likely to be seen in lower energy experiments. Like the EMC data, the E665 results from FNAL with a 490 GeV muon beam (TMC) [2] are far outside the energy region where nuclear effects can be expected to influence hadronization.

Most recently, the HERMES collaboration examined nuclear effects in the scattering of 27.5 GeV positrons from deuterium and nitrogen[17]. The data covered a range of ν from 7 GeV to 23 GeV. The detector could identify π^+'s and π^-'s, but all the other hadrons were characterized only by their electric charges. Besides an attenuation of the hadron spectra, the data also showed a different attenuation of positive and negative hadrons. As suggested in their published results, a complete particle identification will help to clarify this ambiguity.

Most of the existing data were taken with higher beam energies; the energy transfers ν were greater than 7 GeV. As noted by Bialas [23], the high energy data (SLAC) are not accurate enough to determine the energy dependence of the attenuation. One obvious conclusion is that *in addition to increasing their accuracy, it would be of great interest to extend the measurements to lower energies and thus to cover a wider range of the formation time, τ_h.* In addition, the particle identification is weak in the SLAC and HERMES data. Complete PID will make the proposed measurements an even larger step forward.

3.2 Theoretical Work

One of the major outstanding problems in DIS is the theoretical description of hadronization process. Even when the reaction occurs at high momentum transfer where PQCD (perturbative QCD) can be applied, the hadronization process is still dominated by non-PQCD contributions. Hence, phenomenological modeling is unavoidable. The most successful models to date are the Lepto string model [24] [18] and the Venus model [25] [26]. In these models, a fast-moving quark forms a transversely confined color flux tube. Hadrons are generated by a quark-antiquark pair in the color field. These models can predict the multiplicity, energy spectrum, and flavor distribution in the process of hadronization. The confinement caused by the color field explains the limited transverse momentum of the hadrons. Most recently, modified quark fragmentation functions in DIS and the QCD evolution equations were derived in a framework of multiple parton scattering [27]. On the other hand, the Feynman-Field (FF)model [28] [29]. emphasized the description of inclusive data. A fragmentation function was introduced to specify the probability that one of the leading quarks emits a hadron with a certain fraction of its momentum. It is successful in explaining the cross section but fails to describe correlation phenomena.

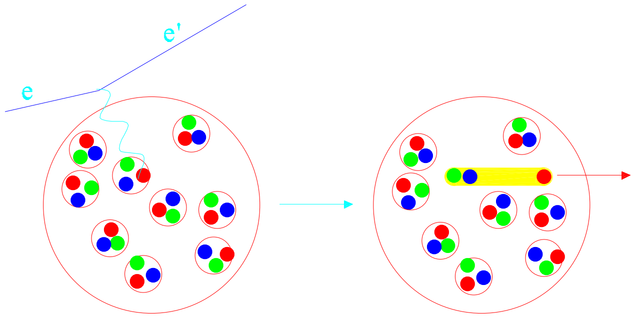

Figure 1: In lepton scattering a string is formed inside the nucleus. The kicked-off moves forward, the diquark is close (in momentum space) to the spectator nucleons.

3.3 The String Models

Venus [25][26] is a model for the fragmentation of a string in a medium of hadrons; final state interactions (FSI) are also included. The code is based on the dual parton model and gluon radiation is not considered. According to the parton model, an energetic lepton delivers a considerable amount of momentum to a quark in the nucleon via a virtual photon. The collision results in a quark-diquark string as shown in Fig. 1. Since the string is formed inside the nucleus, its space-time evolution will be different than if it were in the vacuum. The whole string or the later string fragments may interact with the spectator nucleons.

Lepto [24] [18] is also a relativistic string model for fragmentation. The treatment of several jets is relativistic and it incorporates gluon radiation. Significantly, nuclear effects are not included.

3.4 The Macroscopic Model

The Bialas model is a macroscopic phenomenological model [23] which predicts the hadron attenuation without involving the details of the physics. The calculation is based on 'self-absorption' of the struck quark and the hadron formed from the quark. It folds the quark and hadron probabilities and the cross sections with the density distribution of the target nucleus, thereby including nuclear effects. In describing the DIS of a lepton at a point (b, z) inside the nucleus, the z-axis is the direction of the momentum transfer and b is the transverse dimension. If the characteristic time of the fragmentation is denoted by τ, the probability that the intermediate state at the point (b, z') $(z' \geq z)$ is a quark is given by

$$P_q(z' - z) = exp[(z - z')/\tau],$$

and the probability that it is a hadronic fragment is given by

$$P_h(z' - z) = 1 - P_q(z' - z).$$

Combining the two probabilities, one has the probability that neither the quark nor its fast fragment are absorbed by a single nucleon in the nucleus,

$$S_A(b, z) = 1 - \sigma_q \int_z^\infty dz' \rho_A(b, z') P_q(z' - z) - \sigma_h \int_z^\infty dz' \rho_A(b, z') P_h(z' - z),$$

where σ_q and σ_h are the cross sections for the absorption of the quark or hadron, ρ_A is the nuclear density. The Bialas model treats pions and nucleons equally in the process.

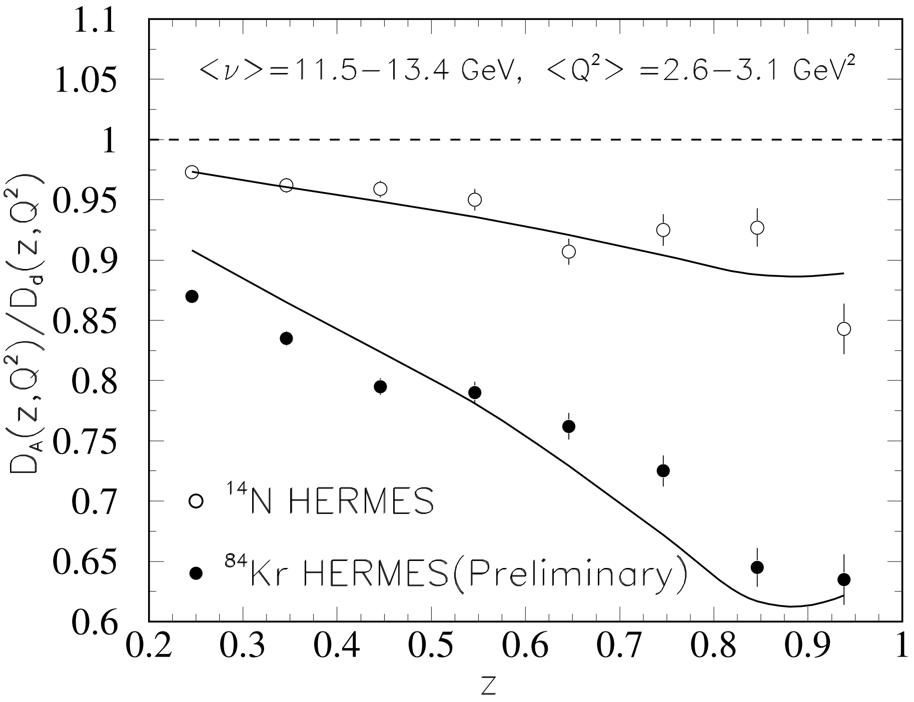

Figure 2: Predicted nuclear modification of jet fragmentation function from Wang model is compared to the HERMES data [17] on ratios of hadron distributions between heavy nuclei and deuterium targets in DIS.

3.5 The Wang Model

The Wang model [27] is based on the fact that the partons generated in DIS will be suppressed as they traverse the nuclear medium. The modified quark fragmentation functions are softened by induced radiation. It is assumed that the modification depends quadratically on the nuclear size. The predicted shape of the $z-$ and $\nu-$dependence agrees well with the experimental data. A remarkable feature of the prediction is the quadratic $A^{2/3}$ nuclear size dependence, as shown in Fig. 2 and Fig. 3 [30].

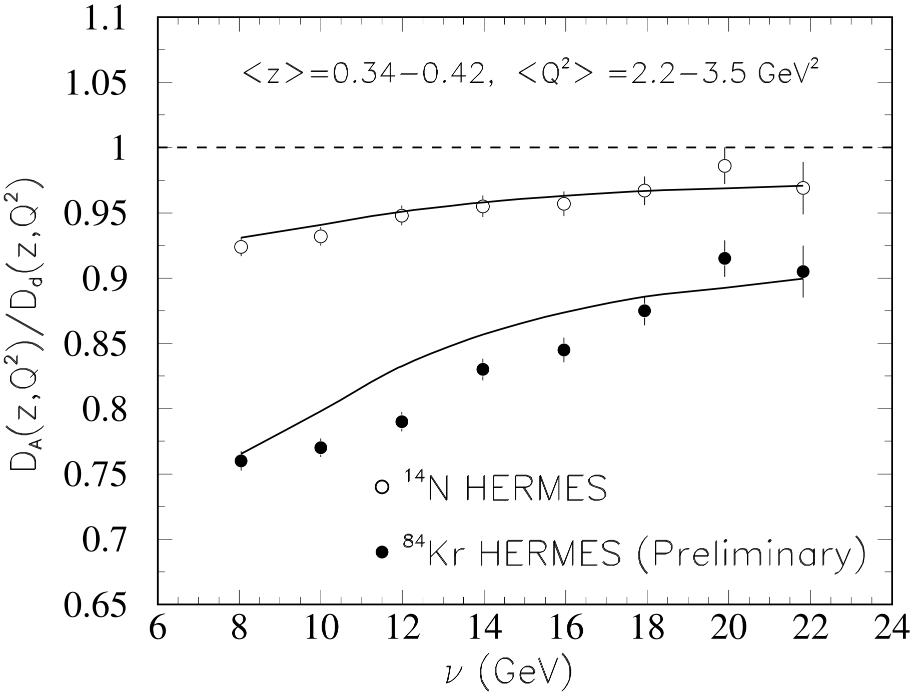

Figure 3: Energy dependence of the nuclear modification from Wang model compared to the HERMES data [17].

4 Experimental Simulation

4.1 Detector Description

The HRSR and HRSL spectrometers will be used for this experiment. The parameters of the two spectrometers are summarized in Table 1.

	HRSR	HRSL
detecting	e^-	$\pi^\pm$, $K^\pm$, p
P_{max} [GeV/c]	3.2	4
θ_{min}	12.5	12.5
acceptance_P [%]	± 4.5	± 4.5
acceptance_H [mrad]	± 28	± 28
acceptance_V [mrad]	± 60	± 60
solid angle [msr]	6	6
$\delta p/p$	10^{-4}	10^{-4}
$\delta\theta_H$ [mrad]	0.6	0.6
$\delta\theta_V$ [mrad]	2.0	2.0

Table 1: Comparison of HRSR and HRSL parameters.

The HRSL was chosen to be the hadron detector for two reasons: it has a higher maximum momentum which permits detection of the hadrons with larger z and it requires a shorter time for a change of the central momentum and the momentum setting will be changed more frequently for the hadron arm. We will detect both positively charged (π^+, K^+ and proton) and negatively charged particles (π^- and K^-) in the HRSL so several reversals of the field will be required. Separation of the various hadronic species will be required. The momentum resolution attainable with the HRSL will be adequate.

The HRSR will be used to detect electrons. The only specific requirement on the HRSR is that it provide good identification of electrons. Its resolution is more than adequate to define the virtual photon with the necessary precision.

4.2 Kinematic Selection

Fig. 4 shows the phase space which can be covered using 6 GeV electrons. The two parallel solid lines (green) show the $Q^2 - \nu$ relationship for W=2 GeV and W=3 GeV. The two dashed lines (blue) show the relationship for for x=0.2 GeV and x=0.6 GeV. The lower bound of the DIS region is normally set at $Q^2 > 1$ (GeV/c)^2 and $W > 2$ GeV to be in the $x-$scaling region and above resonance region. For the case of the present experiment, we also require that $x > 0.2$ in order to suppress events arising from VMD or sea quark contributions. For an inclusive measurement, the available phase space is indicated by the hatched (yellow) area. It is to be noted that Q^2 can be as high as 6 (GeV/c)^2, and W can be as large as 3 GeV.

However, for the semi-inclusive measurement proposed here the available phase space is constrained by the minimum angle at which the hadron detector (HRSL) can be located. We propose to run the experiment at a ν of approximately 4.0 GeV. This will limit the scattered electron energy E_1 to approximately 2.0 GeV. Hence, the three-momentum of the virtual photon q_3 is always greater than E_1. Equivalently, the angle of the hadron arm will always be smaller than that of the electron arm. Consequently, the minimum HRSL angle of 12.5° will place a lower limit on Q^2 as shown in fig. 4 by the short curve (cyan). Three kinematic settings are planned for electron arm corresponding to ν = 3.2 GeV, 4.0 GeV, and 4.4 GeV as indicated by the boxes (red) in Fig. 4. For the electron arm setting of 4.0 GeV, we will use four different hadron arm settings; for the others we will use one. Hence, we will have a total of 6 HRSR-HRSL configurations. The related parameters are listed in Table 2.

The purpose of setting 1 is to explore the z-dependence of the attenuation, that of setting 2 is to explore the charge sensitivity by detecting negatively charged hadrons. For settings 3 and 4, the hadron arm detector will be off the momentum transfer direction and measurements of the P_T-dependence will be made. Setting 5 will be used to study the Q^2-dependence while setting 6 will be used to study the ν-dependence. The data for the kinematics labelled 1 will cover a P_T range from 0 GeV/c to 0.3 GeV/c and will have a statistical uncertainty of about 1%. The data for the kinematics labelled 3, when the

Kin	θ_e (deg.)	ν (GeV)	Q^2 (GeV/c)^2	θ_R (deg.)	θ_h (deg.)	B_h	N_P
1	27.99	4.0	2.81	12.5	12.5	+	5
2	27.99	4.0	2.81	12.5	12.5	−	3
3	27.99	4.0	2.81	12.5	20	+	3
4	27.99	4.0	2.81	12.5	28	+	3
5	41.76	4.4	4.88	12.5	12.5	+	3
6	23.59	3.2	2.81	18.1	18.1	+	3

Table 2: Kinematic parameters of the two detector configuration. θ_e is the electron scattering angle, θ_R is the recoil angle (direction of $\vec{q}$), and θ_h is the angle of hadron arm detector. B_h is the polarity of the magnet of HRSL and N_P is the number of momentum settings.

hadron arm is locating at 20°, will span P_T from 0.3 to 0.5 GeV/c with about 5% statistical precision. The data for the kinematics labelled 4 (28°) will span P_T from 0.45 GeV/c to 0.8 GeV/c with about 10% statistical precision.

4.3 Target

The four targets chosen for this experiment are listed in Table 3, where N_D is the effective number of deuterons per square centimeters. A liquid hydrogen target will also be needed for calibration.

4.4 Simulation

For the purpose of estimating kinematic distributions and rates, the Lepto code was used. However, since we are looking for nuclear effects the Venus code may be more appropriate. Thus, the simulation was performed in two

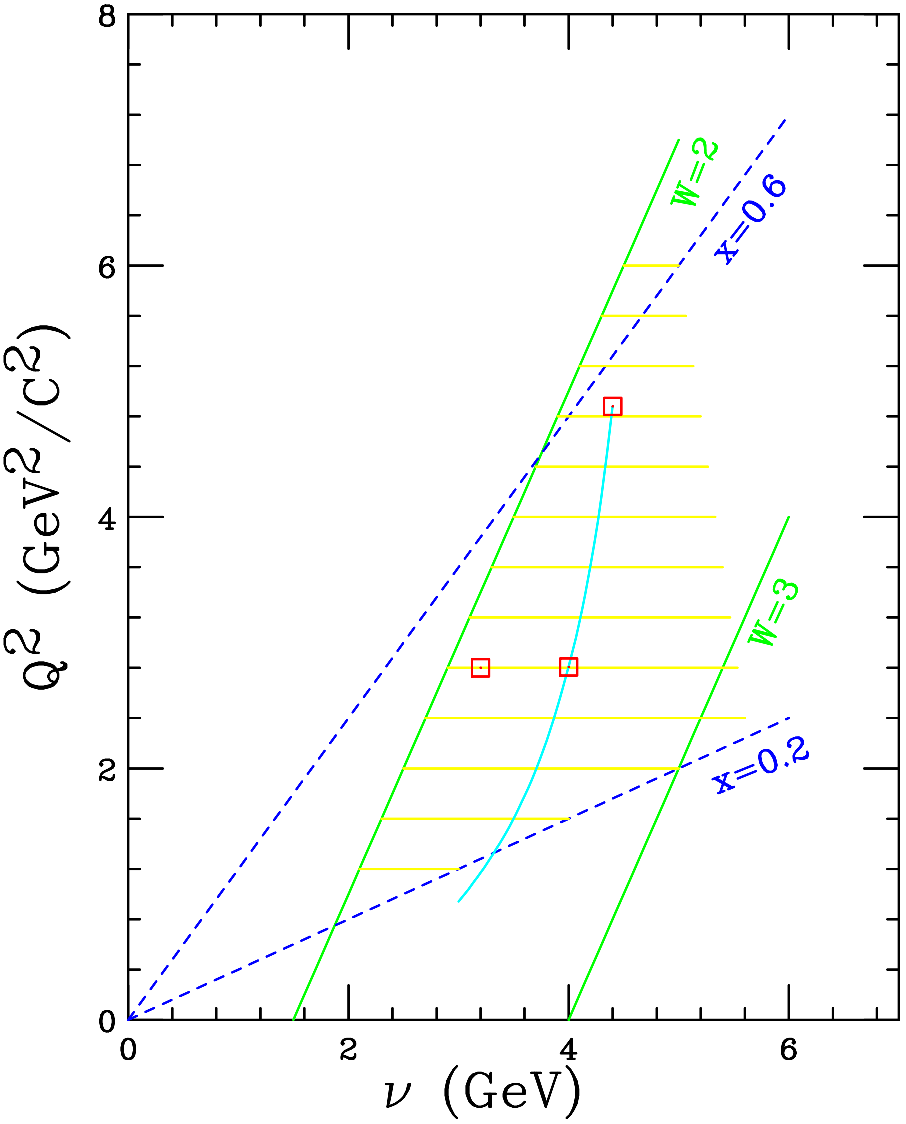

Figure 4: Phase space accessible with an incident electron energy of 6 GeV. The curves are described in the text. The three red boxes indicate the kinematic conditions of the proposed measurements.

target	density (g/cm^3)	thick (cm)	N_D ($10^{23}/cm^2$)	radius (fm)
LD2	0.162	15	7.3	1.4
Carbon	2.265	0.75	5.1	2.6
Copper	8.96	0.072	1.93	4.49
Tungsten	19.3	0.02	1.15	6.38

Table 3: Target parameters.

steps. First, for each setting and target different reaction products were generated. Second, the events were read back by an analyzer which generated histograms for each hadron species with or without the constrain of the angular acceptance of HRSL.

As a cross check to verify the general behavior of the model, simulations assuming a hydrogen target were performed using both the Venus and Lepto codes. The results are shown in Fig. 5. The left side of the figure shows the distributions of individual hadronic species as functions of their polar angle; the right side shows the distributions of their momenta. The shapes of the distributions are, in general, very similar except in the case of the momentum of the proton, where the Lepto code (blue dotted) predicts a larger high energy component.

4.5 Simulation of Deuterium

Simulated spectra were obtained from the Venus code for a deuteron target, the results from which will be used as the standard against which the results from the other targets will be compared. Fig. 6 shows the distributions with respect to polar angle and laboratory momentum. The dotted blue curves represent the total number of hadron production events tagged by an electron while the filled area (yellow) shows the number of (semi-inclusive) events in

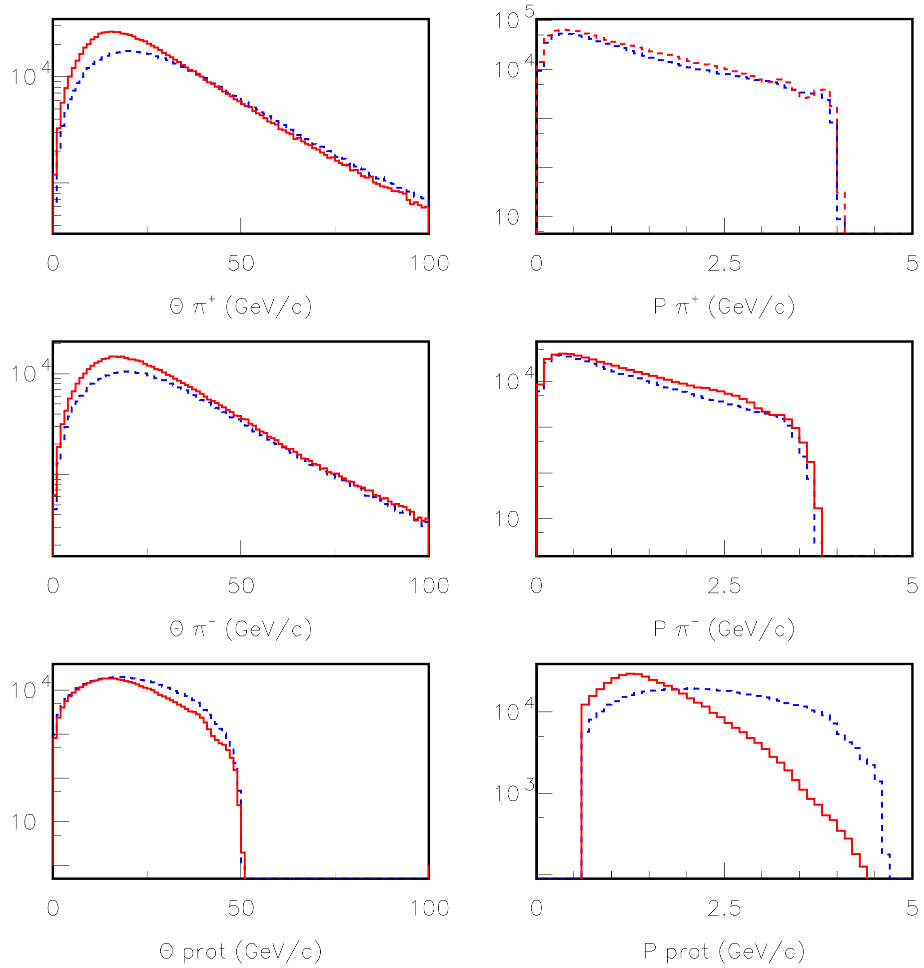

Figure 5: Comparison of hadron spectra (polar angle and momentum) from the Venus and Lepto codes assuming $\theta_e = 27.99°$, ν =4 GeV, a 6 GeV electron beam, and a hydrogen target.

which a hadron is also accepted in the HRSL. One can see that the HRSL hadron detector is located near the maximum of the angular spectra. The momentum of the hadrons extends to about 4 GeV.

Fig. 7 shows the distributions of transverse momentum and x_F for products from a deuterium target. The dotted blue curves represent the total number of hadron production events tagged by an electron while the filled area (yellow) shows the number of (semi-inclusive) events in which a hadron is also accepted in the HRSL. One can see that the accepted hadrons lie predominantly in the low P_T and positive x_F region. This is very important. The positive x_F ensures an observation of current fragmentation while the low P_T limits the measurement to those hadrons possessing momenta nearly parallel to $\vec{q}$. This is also a requirement for observing current fragmentation.

4.6 Rate Estimation

The rate estimation is based on 100 μA beam current and 15 cm liquid deuterium target, which gives a luminosity of 4.56×10^{38} 1/cm^2/sec. Using an inclusive cross section $d\sigma/d\Omega/dE_1$ =6.73 nb/sr/GeV, a momentum bite of 0.18 GeV and a solid angle for each HRS of 6 msr, the electron rate in the HRSR will be about 3.3 kHz, or 11.8M/hour. For a 3-hour run over each momentum interval 35.4 M electron events will be collected.

4.7 Beam Time Request

The beam times assigned to each kinematic setting are listed in Table 4, Table 5, Table 6, and Table 7.

Table 8 is a summary of the time requested for data acquisition, where the time for auxiliary operation related to momentum change, target change, and the relocation of HRS is estimated at 2 hours for each move. The total time is 385 hours or about 16 days. In addition, we estimate needing 2 days for

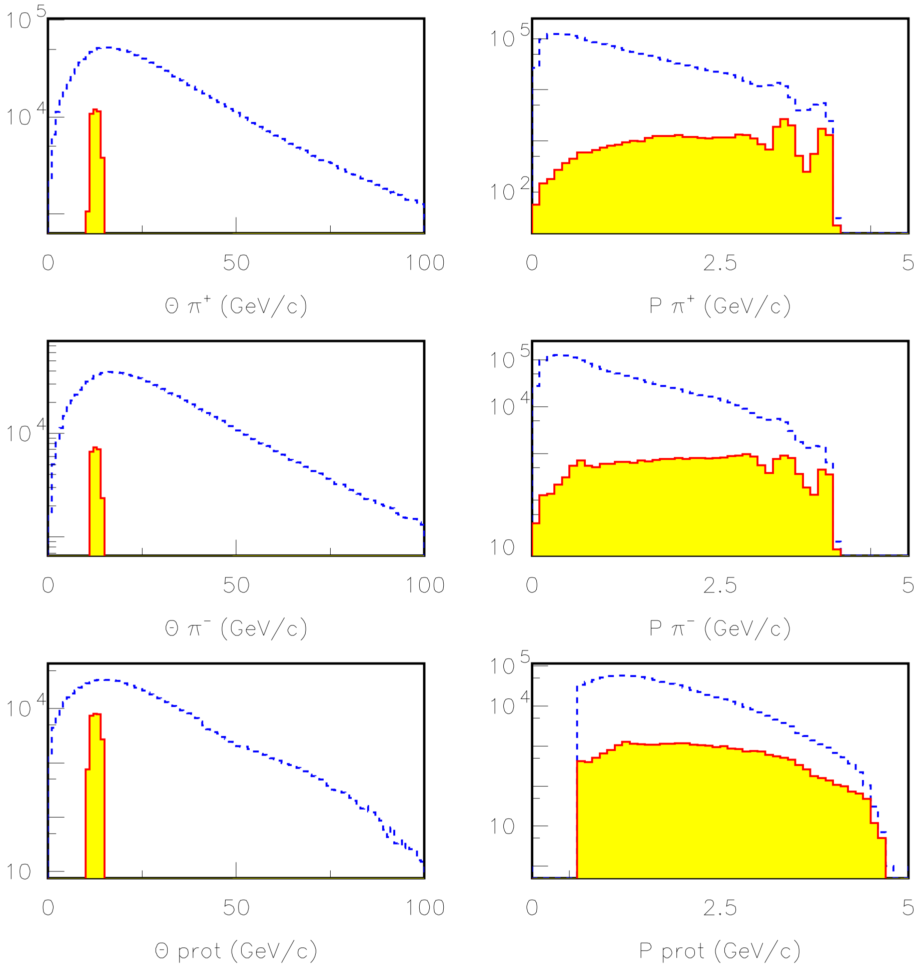

Figure 6: Angle and momentum distributions of π^+, π^-, and proton from a deuterium target. The top curves (blue and dashed) show the spectra of hadrons for events for which an electron was detected in the HRSR only; the shaded area shows those events for which a hadron was detected in the HRSL as well.

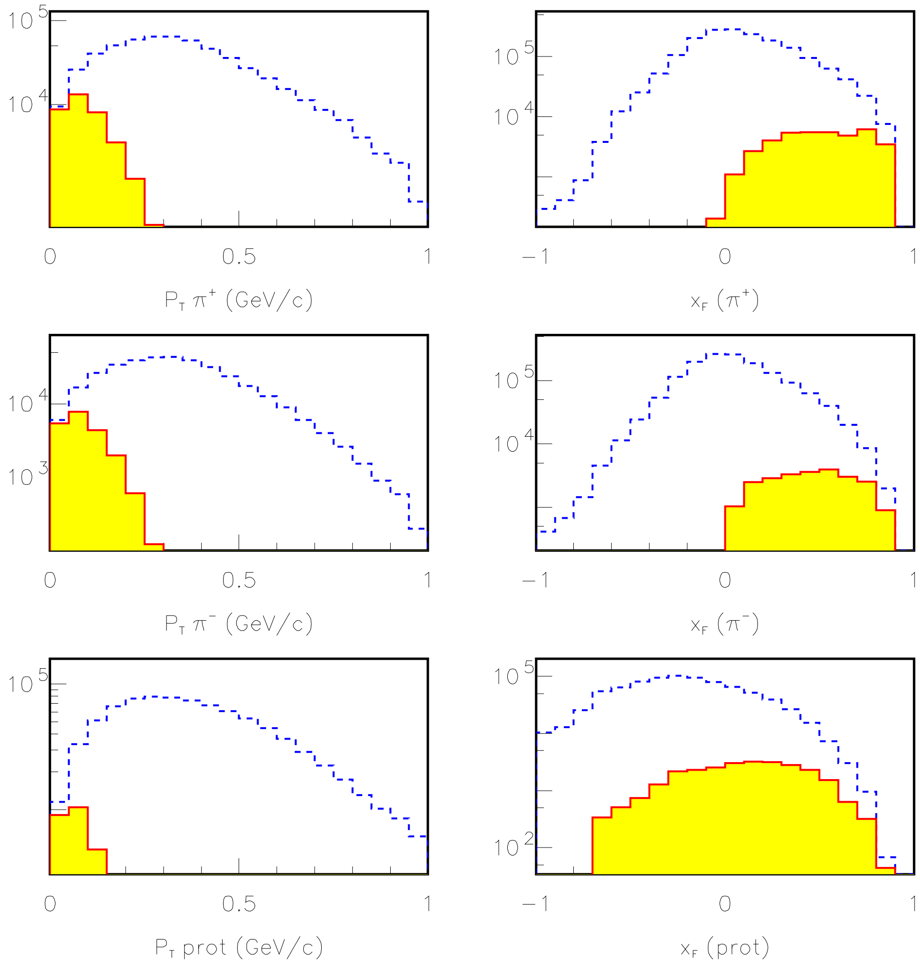

Figure 7: Transverse momentum and x_F of π^+, π^- and proton from deuterium target. The top curves (blue and dashed) show the spectra of hadrons for events for which an electron was detected in the HRSR only; the shaded area shows those events for which a hadron was detected in the HRSL as well.

calibration and set up. Therefore, we are asking for 18 days in total.

P_c (GeV/c)	D (hour)	C (hour)	Cu (hour)	W (hour)
2.230	3	2	5	5
2.430	3	2	5	5
3.197	3	2	5	5
3.498	3	2	5	5
3.828	3	2	5	5
sum	15	10	25	25

Table 4: Beam time assignment for kinematic setting 1. P_c is central momentum to HRSL.

P_c (GeV/c)	D (hour)	C (hour)	Cu (hour)	W (hour)
3.197	3	2	5	5
3.498	3	2	5	5
3.828	3	2	5	5
sum	9	6	15	15

Table 5: Beam time assignment for kinematic setting 2, 3 and 4.

P_c (GeV/c)	D (hour)	C (hour)	Cu (hour)	W (hour)
3.197	6	6	12	12
3.498	6	6	12	12
3.828	6	6	12	12
sum	18	18	36	36

Table 6: Beam time assignment for kinematic setting 5.

P_c (GeV/c)	D (hour)	C (hour)	Cu (hour)	W (hour)
2.430	1	2	3	3
2.670	1	2	3	3
2.921	1	2	3	3
sum	3	6	9	9

Table 7: Beam time assignment for kinematic setting 6.

4.8 Projected Results

Table 9 lists the attenuation ratio for carbon, copper and tungsten from a Venus simulation for π, K and the proton at different values of z. The model generates K^- all at $z < 0.5$, while the threshold of z is taken as 0.5. Hence, there is no K^- listed. The real data for K^- will be a rigorous test of the model.

Two columns of the data in Table 9 are plotted in Fig. 8 for π^+ and proton. The solid curves are calculations from the Bialas model [23], which treats all different hadrons as the same. According to the Venus code, the protons are suppressed more than the pions. The real data will be used to check the two different models. The data will also be used to compare with calculations

Kin	data (hour)	Aux (hour)
1	75	10
2	45	6
3	45	6
4	45	6
5	108	6
6	27	6
total	345	40

Table 8: Overall beam time request for data acquisition.

[31] [32] based on the Wang model as shown in Fig. 9. This model predicts a strong drop for higher z values and for heavier target nuclei. This drop is probably due to the redistribution of the events and the shift of the events from higher z to lower z. The shape of the $z-$dependence will be useful in extracting the formation time as a function of z and ν.

Fig. 10 shows the ν-dependence of hadron attenuation and the Bialas calculation, where curve a (Dashes, blue) is the calculation for A= 12 and $z = 0.65$; curve b (dotted, cyan) is the calculation for A= 64 and $z = 0.65$; and curve c (solid, green) is the calculation for A= 184 and $z = 0.65$. The data points symboled with '+' (blue) are from HERMES, the data point (yellow) near 10 GeV is from SLAC data on carbon. The predicted data for the proposed experiments for π^+ is shown with red diamonds ($z = 0.65$ and carbon), red circles (z=0.65 and copper) and red boxes (z=65 and tungsten) at $\nu = 3.2$, 4 and 4.4 GeV. The two data points at $\nu = 3.2$ and 4 GeV are at the same Q^2 which will reflect the $\nu-$dependence of the formation time. The two data points at $\nu = 4.0$ and 4.4 GeV have a big difference of Q^2, so they can be used to study the Q^2-dependence of the attenuation.

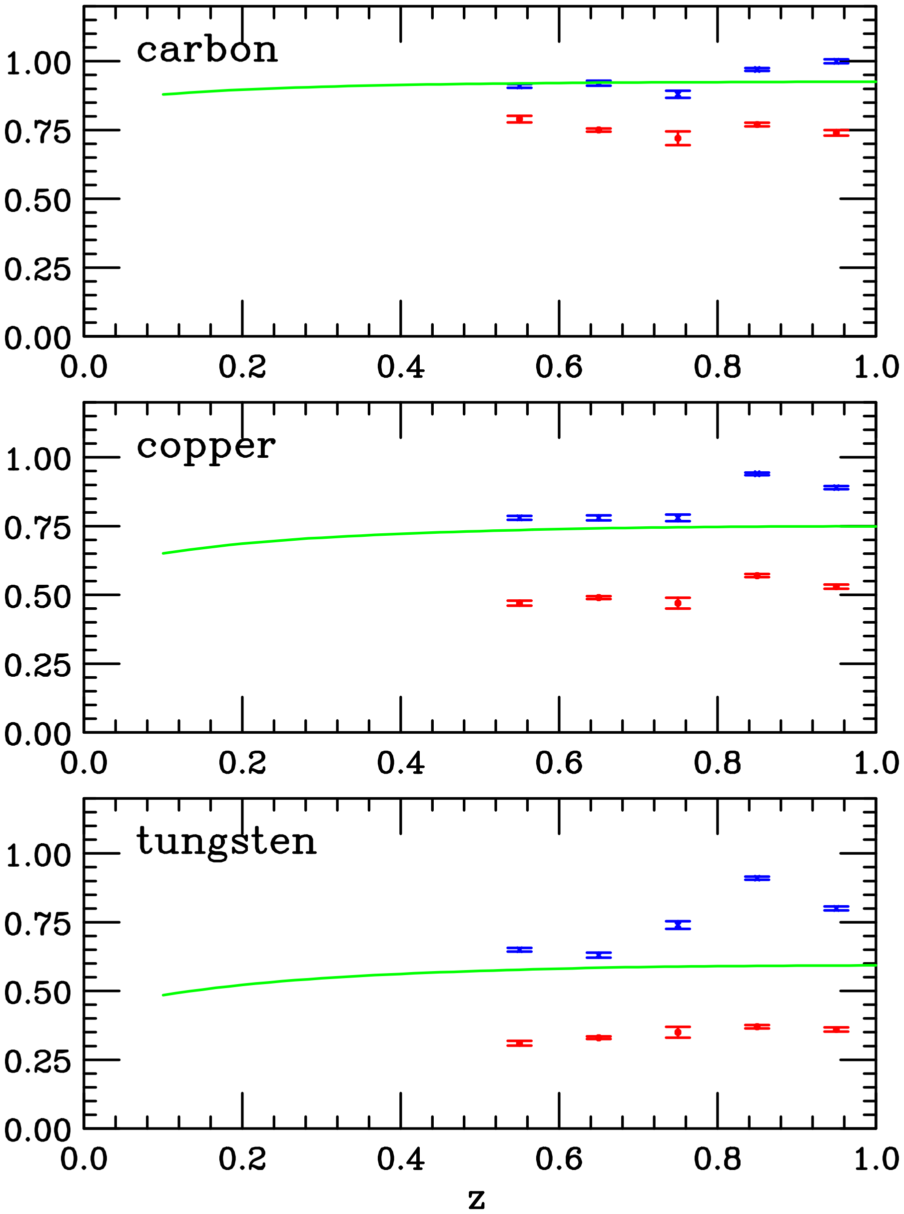

Figure 8: Attenuation of π^+ (blue x) and proton (red o) in carbon (top), copper (central) and tungsten (bottom) as a function of z for $\nu = 4$ GeV. A cut of $x_F > 0$ has been applied.

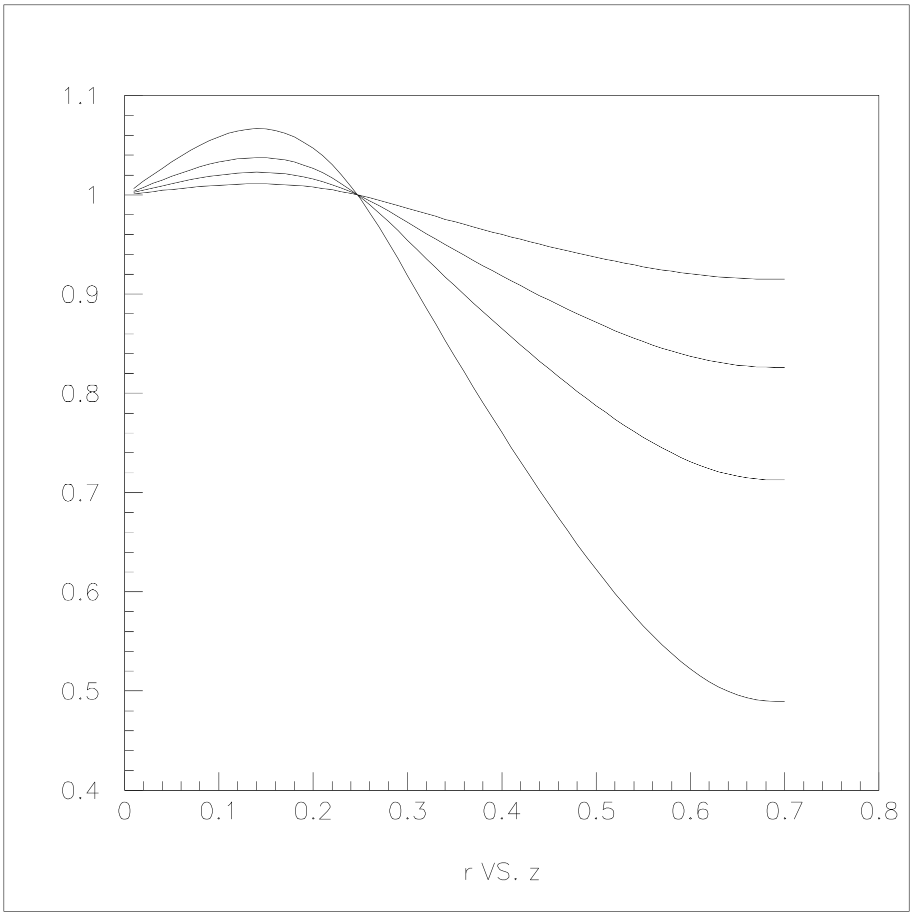

Figure 9: Predicted behavior from the Wang model for the z-dependence of the hadronic multiplicity ratio for $\nu = 5$ GeV and $Q^2 = 2$ (GeV/c)^2. The curves, from the top to the bottom, are for nitrogen, argon, krypton and gold.

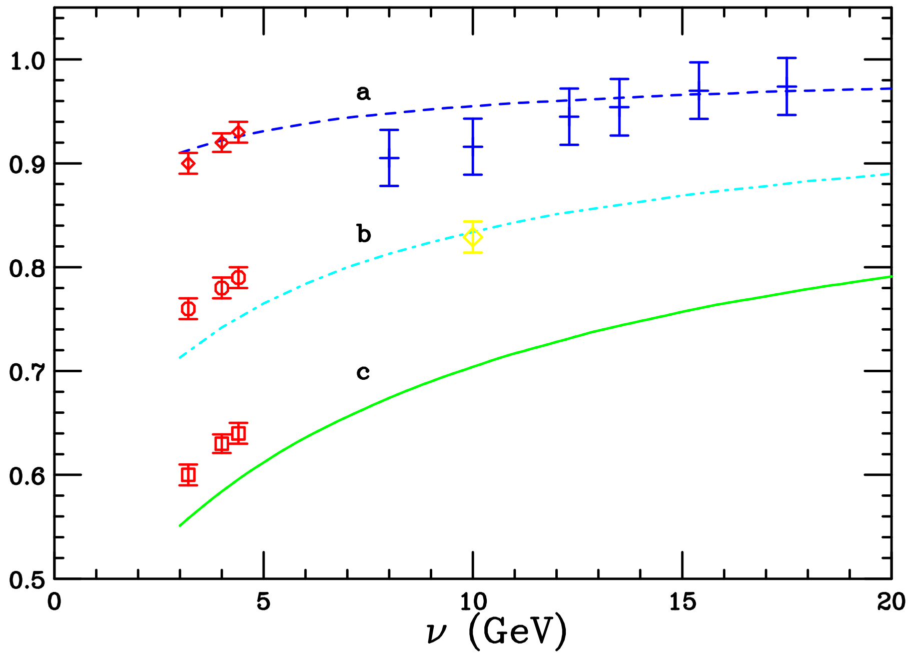

Figure 10: Attenuation of hadron as a function of ν, curve a (dashes, blue) for $z = 0.65$ and carbon, curve b (dash-dotted, cyan) for $z = 0.65$ and copper, curve c (solid, brown) for $z = 0.65$ and tungsten, The three data points (red) at 3.2, 4 and 4.4 GeV are projected for π^+ at $z = 0.65$.

t	z	π^+	K$^+$	proton	π^-
C	.55	.91±.007	.98±.018	.79±.012	
	.65	.92±.009	1.±.020	.75±.006	
	.75	.88±.013	1.±.081	.72±.025	.97±.018
	.85	.97±.005	.94±.007	.77±.007	.96±.007
	.95	1.±.007		.74±.010	1.±.013
Cu	.55	.78±.007	.86±.016	.47±.009	
	.65	.78±.009	.78±.017	.49±.005	
	.75	.78±.012	1.±.070	.47±.020	.94±.017
	.85	.94±.005	.84±.007	.57±.006	.90±.007
	.95	.89±.006		.53±.008	1.±.014
W	.55	.65± .007	.67± .017	.31± .009	
	.65	.63± .009	.65± .018	.33± .005	
	.75	.74± .014	1.± .085	.35± .020	.73± .018
	.85	.91± .006	.70± .008	.37± .006	.83± .009
	.95	.80± .007		.36± .008	1.± .017

Table 9: Hadron attenuation for carbon (C), copper (Cu) and tungsten (W) as a function of z for setting 1 and 2 ($\nu = 4$ GeV) and $x_F > 0$.

5 Summary

We propose to study current fragmentation using deep inelastic electron scattering, $A\,(e, e'[\pi, K, p])\,X$ with 6 GeV electrons and deuterium, carbon, copper and tungsten targets. Separate fragmentation functions will be extracted for each hadronic species. Dependencies on Q^2, x, ν, P_T, z and A will be obtained. The high statistics, high resolution results will shed light on the formation time in hadronization, quark re-scattering in the nuclear medium, as well as a possible observation of LPM effect. The data with $\nu = 3$ and 4 GeV will serve as an input to the interpretation of the RHIC data.

We request 18 days beam time, of which 2 days will be used for detector set up and calibration; 16 days will be devoted to data acquisition.

A Comparison to Other Experiment

The general physics issues to be addressed with the proposed experiment parallel those of an approved Hall-B proposal, E02-104 [32]. However, the highly specified kinematic selectivity and high luminosity make the Hall-A experiment a necessary complement to the Hall-B experiment, especially at relatively high Q^2 and large z.

Due to the small acceptance of HRS, data can be taken at very small bin of both Q^2 and ν. By locating HRS at specific angle, we can select the events at higher Q^2 without being overwhelmed by much more probable low Q^2 processes. The small cross section can be compensated by the high luminosity at Hall-A. With this feature, it will be possible to check the variation of the attenuation with Q^2 and x, to determine whether it is really as small as predicted. On the other hand, the current fragmentation study at low energy requires hadrons with large z; i.e., hadrons with momenta above 2 GeV/c. However, the hadron spectra peak at low momentum. The second HRS will be used to selectively isolate events involving energetic hadrons in the final state. Similarly, it will be possible to select data at larger, well defined values of P_T by changing the angular orientation of HRSL. This will be of fundamental importance to the study of QCD color confinement and quark re-interaction. The high resolution will enable us to optimize the kinematics to be sensitive to possible QCD effects which depend on Q^2 and ν.

Since hadrons of different types with large momentum are involved, we need to compare the differences in hadronization for pions, kaons and protons. Therefore, particle identification will play an important role. The HRS to be used for hadron detection is equipped with an aerogel Cherenkov detector and a RICH detector (CsI-freon) which will offer good separation of kaon from pion over the full momentum range[33]. In addition, time-of-flight will also be used.

References

[1] J. Ashman *et al.*, Z Phys. **52**, 1 (1991).

[2] M. R. Adams *et al.*, Phys. Rev. D **50**, 1836 (1994).

[3] M. Johnson, B. Kopeliovich, and A. V. Tarasov, Phys. Rev. C **63**, 035203 (2001).

[4] J. D. Bjorken, in Current Induced Reactions, Lecture Notes Physics 56, Ed. J.G. Korner et al., 1975.

[5] V. Eckardt *et al.*, Phys. J1N **11**, 56 (2002).

[6] Q. Liu and T. A. Trainor, hep-ph/0301214 **1**, 1 (2003).

[7] A. Drees, nucl-ex/0105019, 2001.

[8] K. Adcox *et al.*, Phys. Rev. Lett. **88**, 022301 (2002).

[9] L. Landau and I. Pomeranchuk, Dikl. Akad. Nauk SSSR **92**, 92 (1953).

[10] A. Migdal, Phys. Rev. **103**, 1811 (1956).

[11] M. Gyulassy and X.-N. Wang, Nucl. Phys. B **420**, 583 (1994).

[12] X.-N. Wang *et al.*, Phys. Rev. D **51**, 3436 (1995).

[13] D. Perkins, Introduction to high energy physics, 1987, 3rd edition.

[14] Particle property data booklet, Phys. Lett **B239**, 241 (1990).

[15] P. Renton and W. S. C. Williams, Ann. Rev. of Nucl. and Part Scin **31**, 193 (1981).

[16] T. Sloan, Physics Report **162**, 46 (1988).

[17] A. Airapetian *et al.*, Eur. Phys. J. C. **20**, 479 (2001).

[18] B. Ansderson *et al.*, Phys Rep **97**, 31 (1983).

[19] B. Kopeliovich *et al.*, nucl-th/9607036, 1996.

[20] R. Baier, D. Schiff, and B. G. Zakharov, Annl. Rev. of Nucl. and Part. Science **50**, 37 (2000).

[21] X.-N. Wang, Phys. Rev. C **63**, 054902 (2001).

[22] L. S. Osborne *et al.*, Phys. Rev. Lett. **40**, 1624 (1978).

[23] A. Bialas, Phys. Lett **133B**, 241 (1983).

[24] G. Ingelman, A. Edin, and J. Rathsman, code Lepto, http//www3.tsl.uu.se/thep/lepto., 1996.

[25] K. Werner and P. Koch, Z. Phys. C **47**, 215 (1990).

[26] K. Werner, Venus code, private communication.

[27] X. Guo and X.-N. Wang, Phys. Rev. Lett **85**, 3591 (2000).

[28] R. Field and R. P. Feynman, Nucl. Phys. B **136**, 1 (1978).

[29] R. Field and R. P. Feynman, Phys. Rev. D **15**, 2590 (1977).

[30] E. Wang and X.-N. Wang, hep-ph/0202105, 2002.

[31] X.-N. Wang, Wang model calculation, private communication.

[32] W. Brooks *et al.*, Jlab proposal E02-014, 2002, quark propagation through cold QCD matter.

[33] E. Voutier and K. de Jager, Hall A status report, 2002.